Physics Letters A 375 (2011) 918–921

Contents lists available at ScienceDirect

Physics Letters A

www.elsevier.com/locate/pla

Optical switching and logic gates with hybrid plasmonic–photonic crystal nanobeam cavities

Ivan S. Maksymov

Nonlinear Physics Centre, Research School of Physics and Engineering, Australian National University, Canberra ACT 0200, Australia

ARTICLE INFO

Article history:
Received 10 December 2010
Accepted 22 December 2010
Available online 29 December 2010
Communicated by V.M. Agranovich

Keywords:
Photonic crystal cavity
Plasmonic nanostructure
Optical switching device
Optical logic gate

ABSTRACT

We propose a hybrid resonance architecture in which a plasmonic element is coupled to a silicon-on-insulator photonic crystal nanobeam cavity operating at telecom wavelengths. It benefits from the combined characteristics of the photonic cavity and the plasmonic element, and exploits the unique properties of Fano resonances resulting from interactions between the continuum and the localized cavity states. As confirmed through 3D time-domain simulations, a strong cavity mode damping by the plasmonic element offers mechanisms of controlling a probe signal propagating in the nanobeam. It makes possible to create optical switching devices and logic gates relying on any optical nonlinear effect.

1. Introduction

Optical nanocavities are increasingly gaining interest in nanophotonics and nanoplasmonics due to their capability of confining light into ultrasmall volumes essential for the control of light-matter interaction at the nanoscale [1]. Recent theoretical and experimental advances in this area are directed toward developing hybrid plasmonic–photonic nanocavities that benefit from both the original cavity characteristics and the plasmonic features of the metallic elements [2]. A representative example of the hybrid cavity architecture are solid-state nanocavities with a metallic coating [3]. In comparison with conventional photonic crystal (PhC) cavities or nanopillars, the metallic coating offers smaller mode volumes and a suppression of off-resonant leaky modes, which boosts the light-matter interaction and opens new routes for the control of the coupling between a light source with the cavity mode [4,5].

The main drawback of metal-coated cavities is the inevitable nonradiative decay rate induced by metallic losses that significantly worsen the performance of the device. It motivates a search for hybrid architectures that provide appropriate modal conversion and light-coupling conditions ensured by the use of intermediate resonator structures [6]. For instance, PhC nanocavities with a tapered plasmonic nanotip antenna [7,8] and a plasmonic nanoparticle [9] precisely placed on its backbone have been proposed. They preserve the characteristics of the original PhC cavities such as a high quality factor Q and the ability to host a quantum emitter inside it. On the other hand, they benefit from the unique features of the metallic element such as the ability to support surface plasmons polaritons and confine light into ultrasmall volumes much beyond its free-space wavelength. However the physics and the operational principles of hybrid systems with an external plasmonic element may be fundamentally different. The cavity mode of the PhC nanocavity equipped with a metallic nanoantenna is strongly damped due to the presence of the metallic base of the antenna. It ensures more efficient coupling of an external light source with the modes of the nanoantenna [7,8] and allows tuning the field enhancement at the nanoantenna tip. In contrast, the modal field of the cavity with a metal particle on its backbone is enhanced and shifted from the center of the PhC slab to its surface. This feature is highly advantageous for all applications where external emitters or other types of materials placed on the top of the PhC structure have to coupled evanescently with the cavity mode [9].

In this Letter, we focus ourselves on a hybrid plasmonic–photonic architecture with a plasmonic element intended for the damping of the fundamental cavity mode. We report the design and the full-vectorial 3D finite-difference time-domain (FDTD) simulations of a hybrid plasmonic–photonic architecture consisting of a silicon-on-insulator nanobeam cavity and a cylindrical plasmonic nanoantenna placed in the close proximity to the top surface of the cavity. In contrast to the system recently introduced by de Angelis et al. [7,8], the role of the nanoantenna in the investigated device is reversed. In our device the nanoantenna controls the optical properties of the PhC cavity in the same way as a pump laser beam controls the response of PhC all-optical switches relying on nonlinear optical effects. Our full-vectorial 3D FDTD simulations demonstrate that the fundamental cavity mode is strongly damped

E-mail address: mis124@physics.anu.edu.au.

0375-9601/$ – see front matter
doi:10.1016/j.physleta.2010.12.054

when the nanoantenna is present. It suggests the application of the observed control mechanism to a switching device and logical NOT and AND gates.

2. Design and numerical method

High quality and small mode volume optical nanocavities are required for the realization of PhC all-optical switches, which are expected to replace their electrical counterparts in information processing [10]. Despite considerable progress, PhC switches are still immature due to their relatively large size and power consumption [11]. That is why much attention is now given to all-optical switches based on photonic nanobeam cavities [12]. These cavities possess a small mode volume comparable to $(\lambda/n)^3$ (λ is the wavelength of light, n is the refractive index), implying a strong decrease in the power density required for the switching. The footprint of the nanobeam based devices is much lower than that of conventional PhC cavities, which makes the former especially attractive for the application in on-chip photonic data communication systems.

The investigated PhC nanocavity consists of a 260 nm silicon core layer supported by a 1 μm silica substrate. The one-dimensional (1D) periodic structure comprises a single row of circular air holes in a 500 nm wide photonic wire waveguide with a lattice constant $a = 375$ nm and a radius $r/a = 0.28$. The periodic photonic structure is designed such that the center of its large stop-band is at about 1550 nm for the TE polarization [13]. The regions within the cavity and between the mirrors are tapered by means of holes with different radii. The tapers allow reducing and recycling mirror losses due to out-of-plane scattering induced by optical impedance mismatch [14]. A schematic drawing of the cavity with a six-hole mirror and tapers is presented in Fig. 1. The inset shows a top view of the nanocavity with the positions of the source and field monitors used in the FDTD simulations. We notice that the whole structure is very compact and has a footprint of about 5 μm^2.

Calculations of transmission spectra and spatial distributions of the electromagnetic fields are performed by means of a 3D FDTD method, which consists of solving the Maxwell's equations in space and time without mathematical approximations [15]. The leapfrogging in time followed by implementation of staggered spatial grids leads to an accurate evaluation of the relevant derivatives via finite differences. Absorption of the field components approaching the boundaries of the spatial grids is guaranteed by implementation of the Convolution-Perfectly-Matched-Layers (CPML) absorbing boundary conditions [15]. A bandpass Gaussian pulse is employed at $t = 0$ as the initial condition. The numerical simulation of the propagation of this pulse reproduces the conditions of the full-scale study, i.e. a single run of the FDTD program results in time-domain data containing information about the propagation of the electromagnetic fields at wavelengths between 0.5 eV and 1.5 eV. Transmission spectra are next obtained from these time-domain data using a high-resolution Fourier transformation. Spatial distributions of the electromagnetic field are obtained simultaneously by performing a running Fourier transformation at every gridpoint of the computation domain for each frequency of interest.

The plasmonic nanoantenna is implemented as a gold $H_a = 500$ nm long cylinder with the diameter $D = 135$ nm. The dielectric function of gold is based on a Drude model fit for the published optical constants of gold [16]. The diameter of the nanoantenna is chosen such that the facet of the cylinder covers the defect in the periodic structure of the nanobeam (see the inset in Fig. 1). According to auxiliary calculations, the height of the nanoantenna can be chosen arbitrarily because the role of the nanoantenna consists in the outcoupling of light from the cavity and its conversion to free-propagating optical radiation. A discussion related to the efficiency of this conversion can be found elsewhere [17]. We anticipate using metallic antennas with other shapes and constructive embodiments such as metallic spheres that can be manipulated by means of laser optical tweezers [18,2].

3. Results and discussion

We calculate transmission spectra of the nanobeam cavity with and without the nanoantenna according to the method described in the above. Fig. 2(a) shows the calculated spectra of the PhC cavity without the nanoantenna (red-solid curve) and with the nanoantenna that is closely approached to the top interface of the cavity (black-dashed line). An overview of the spectrum of the isolated cavity reveals a strong resonance peak at ~ 0.826 eV corresponding to the fundamental TE mode. This peak has a strongly asymmetric Fano-type lineshape [19,20] taking place due to the Fano quantum interference effect describing the interaction between two coupled channels in a scattering problem. In the present study, the two interfering signals correspond to light that is directly (nonresonantly) transmitted through the nanobeam 1D periodic structure and detected by the monitors, which gives rise to a small continuum background signal, and light that is resonantly coupled to the cavity mode and then retransmitted toward the monitors. It is worth to mention that the physical picture of the Fano resonance in 1D periodic structures is even more complicated due to the non-local coupling that provides a scattered wave with the possibility of bypassing the cavity [21].

The peak in the spectrum calculated in the presence of the nanoantenna [black-dashed line in Fig. 2(a)] has the shape of a reversed Lorentzian. Resonances with this lineshape can be also explained by means of the Fano model.

In order to provide proof that the observed resonances can be classifies as the Fano resonances, we fit the calculated transmittance data with the Fano lineshape and analyze the obtained results in terms of the dimensionless asymmetry parameter q accounting for the ratio between resonant and nonresonant transition amplitudes. According to [22], we use a Fano-fit formula:

$$F(E) = A(E) + F_0 \frac{[q + 2(E - E_0)\Gamma]^2}{1 + [2(E - E_0)\Gamma]^2}, \tag{1}$$

where E_0 is the resonance energy of the cavity mode, Γ is the resonance linewidth, F_0 is a constant factor and $A(E)$ is a cubic polynomial that improves the fit of the tails of the resonance peaks. By analyzing Eq. (1) we see that the values of $|q|$ of the order of unity correspond to the situation of comparable resonant and nonresonant pathways in the transmission process; strongly asymmetric resonances are observed in this case. Large $|q|$ mean that the resonant transmission dominates over the direct one; the observed lineshape tends towards a symmetric Lorentzian. Finally, small $|q|$ values result in reversed Lorentzian lineshapes corresponding to the anti-resonance [20].

The obtained Fano best-fits are shown in Fig. 2(b) and (c). For the nanocavity without the nanoantenna, we obtain $q = 0.152$ and the corresponding quality factor $Q = E_0/\Gamma \approx 755$. In the presence of the nanoantenna the fit produces $q = 0.0025$ and $Q \approx 95$. These results explain the impact of the plasmonic nanoantenna on the resonance properties of the nanocavity. When the nanoantenna is absent, the light detected by the monitors (see the inset in Fig. 1) mainly comes from the cavity that ensures the domination of the resonant transmission over the nonresonant one. When the nanoantenna approaches the top surface of the cavity, the contribution of the cavity into the monitored time-domain signal drastically decreases due to a strong mode damping by the nanoantenna. It results in the predominance of the nonresonant transmission and, according to the Fano model, leads to a reverse

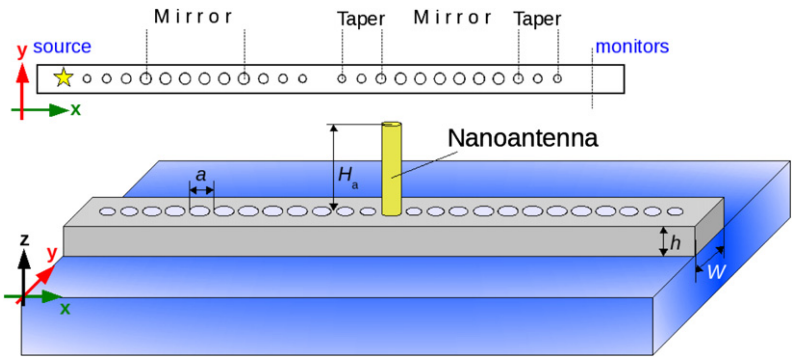

Fig. 1. Perspective view of the silicon-on-insulator nanobeam cavity with a plasmonic nanoantenna. The cavity is formed by two tapered mirrors consisting of air holes in a silicon rectangular nanowire (gray region, width $W = 500$ nm and height $h = 260$ nm) with a silica substrate (blue region). The distance between the holes of the mirrors is $a = 375$ nm and the radius of the holes is $r = 0.28a$. The radii of the holes in the tapers are $0.24a$, $0.22a$ and $0.19a$, respectively. The diameter and the height of the gold nanoantenna are $D = 135$ nm and $H_a = 500$ nm, respectively. The inset shows the top view of the cavity. The position of the source and the field monitors used in the FDTD simulation is indicated. (For interpretation of the references to color in this figure legend, the reader is referred to the web version of this Letter.)

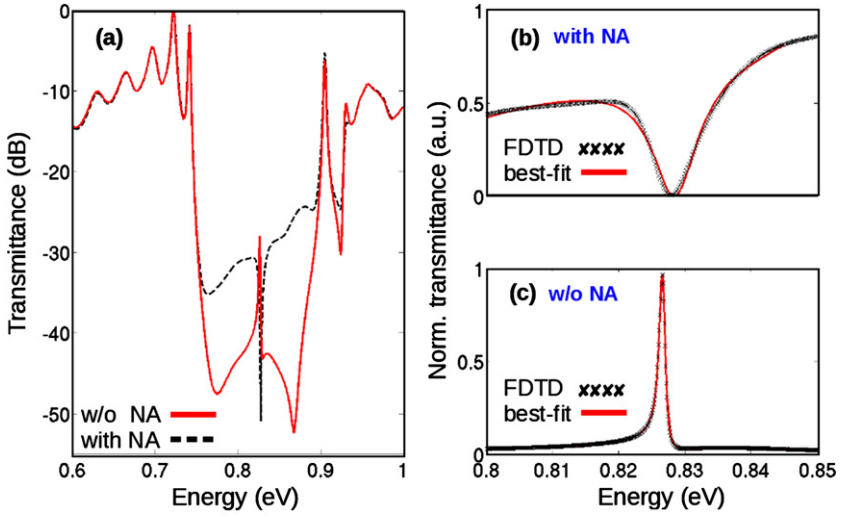

Fig. 2. (a) Calculated transmission spectra of the PhC wire nanocavity without the nanoantenna (red-solid line) and with the nanoantenna approached to the top surface of the cavity (black-dashed line). The spectra are normalized such that their maxima correspond to 0 dB. (b), (c) Calculated spectra normalized to unity (crosses) and the corresponding Fano best-fits (solid lines). (For interpretation of the references to color in this figure legend, the reader is referred to the web version of this Letter.)

Lorentzian lineshape of the resonance peak. This prediction is confirmed by the FDTD simulation. An eight-fold decrease in Q in the presence of the nanoantenna is attributed to the metal losses induced by the nanoantenna.

According to the fit, the resonant energy of the cavity without the nanoantenna is $E_0 \approx 0.8266$ eV whereas in the presence of the nanoantenna it slightly increases up to $E_0 \approx 0.8285$ eV. The distance between the peaks is comparable with the best-fit resonance linewidth for the cavity without the nanoantenna. However, if the nanoantenna is absent, the maximum of the transmission peak averages about -30 dB whereas the minimum of the reversed Lorentzian peak (cavity with nanoantenna) is at about -50 dB. It results in a contrast of about 20 dB, a feature that is strongly related to the Fano interference effect. This funding allows using the present device as a switch in which the cylindrical or any other metallic nanoantenna plays the role as a strong pump beam controlling a probe signal propagating in the PhC nanobeam.

We demonstrate the switching performance of the device by simulating the propagation of a probe signal in the nanobeam. We calculate the field intensities in the nanobeam with and without the nanoantenna. One of the ends of the nanobeam is excited with a continuous wave (CW) oscillating at $E = 0.8266$ eV corresponding to the maximum of the transmission peak in the spectrum of the cavity without the nanoantenna. The calculated field intensities are presented in Fig. 3. The intensity profile corresponding to the cavity without the nanoantenna [Fig. 3(a), (b)] has a bright spot at the center demonstrating the localization of the field in the cavity region. The calculation for the cavity with the nanoantenna [Fig. 3(c), (d)] carried out at the same energy shows that the light travelling into the entrance of the nanobeam penetrates the mirror of the cavity but is completely reflected backwards according to the spectral calculations.

The analysis of the calculated field profiles confirms the capability of the proposed hybrid plasmonic–photonic architecture to perform as a switch controlled by the metallic nanoantenna. As far as we know, the observed switching contrast, defined as a contrast between the maximum and the minimum of the transmission peaks, is over two times larger than that reported for state-of-the-art PhC all-optical switches [11].

The device can also perform as a NOT or an AND logic gate. The NOT operation corresponds to a high output signal when the nanoantenna is absent and it switches to low when the

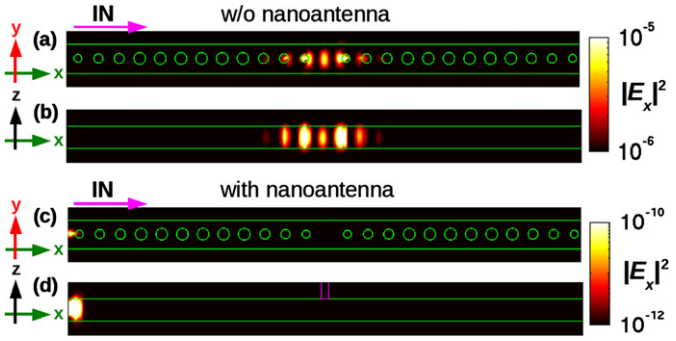

Fig. 3. Calculated $|E_x|^2$ field profiles at $E = 0.8266$ eV in the XY and XZ planes of the nanobeam cavity with (a), (b) and without (c), (d) the nanoantenna. The contours of the nanobeam and the nanoantenna are indicated with the green and magenta lines, respectively. The arrow denotes the propagation direction of the probe signal. Notice the change in the colorscales when the nanoantenna is added. (For interpretation of the references to color in this figure legend, the reader is referred to the web version of this Letter.)

nanoantenna closely approaches the top surface of the cavity. The AND operation corresponds to the case when the output is low if the nanoantenna is absent and it is high in its presence.

4. Conclusions

We have presented a numerical study of the hybrid plasmonic–photonic architecture based on a silicon-insulator photonic-crystal nanobeam cavity equipped with a metallic nanoantenna. The nanoantenna, which can be implemented as a metallic nanotip (e.g. a tip of an atomic force microscope (AFM) [23]) or a metallic particle manipulated by laser optical tweezers, strongly damps down the fundamental cavity mode and performs similarly to a laser pump beam controlling a probe signal propagating in the PhC nanobeam. As confirmed by the full-vectorial 3D time-domain simulations, this control mechanism opens new routes for implementing optical switching devices and logic gates. Our fundings can be additionally used to improve the device presented in [7,8]: the substitution of the PhC cavity by the nanobeam cavity will considerably decrease the footprint of the device and allow its integration with other on-chip photonic components.

Acknowledgements

The author thanks Prof. Yuri Kivshar and Dr. Andrey Miroshnichenko for the support and useful discussions. This work was supported by the Australian Research Council.

References

[1] R.B. Wehrspohn, H.-S. Kitzerow, K. Busch (Eds.), Nanophotonic Materials: Photonic Crystals, Plasmonics and Metamaterials, Wiley-VHC, 2008.
[2] G. Cojoc, C. Liberale, R. Tallerico, A. Puija, M. Moretti, F. Mecarini, G. Das, P. Candeloro, F. De Angelis, E. Di Fabrizio, in: A. Diaspro (Ed.), Nanoscopy and Multidimensional Optical Fluorescence Microscopy, CRC Press, 2010, pp. 15-1–15-30.
[3] T. Lund-Hansen, S. Stobbe, B. Julsgaard, H. Thyrrestrup, T. Sünner, M. Kamp, A. Forchel, P. Lodahl, Phys. Rev. Lett. 101 (2008) 113903.
[4] M.P. Nezhad, A. Simic, O. Bondarenko, B. Slutsky, A. Mizrahi, L. Feng, V. Lomakin, Y. Fainman, Nat. Photon. 4 (2010) 395.
[5] I.S. Maksymov, M. Besbes, J.P. Hugonin, J. Yang, A. Beveratos, I. Sagnes, I. Robert-Philip, P. Lalanne, Phys. Rev. Lett. 105 (2010) 180502.
[6] A. Belarouci, T. Benyattou, X. Letartre, P. Viktorovitch, Opt. Express 18 (2010) A381.
[7] F. de Angelis, M. Patrini, G. Das, I. Maksymov, M. Galli, L. Businaro, L.C. Andreani, E. di Fabrizio, Nano Lett. 8 (2008) 2321.
[8] F. de Angelis, G. Das, P. Candeloro, M. Patrini, M. Galli, A. Bek, M. Lazzarino, I. Maksymov, C. Liberale, L.C. Andreani, E. di Fabrizio, Nature Nanotech. 5 (2010) 67.
[9] M. Barth, S. Schietinger, S. Fischer, J. Becker, N. Nüsse, T. Aichele, B. Löchel, C. Sönnichsen, O. Benson, Nano Lett. 10 (2010) 891.
[10] M. Belotti, J.F. Galisteo López, S. de Angelis, M. Galli, I. Maksymov, L.C. Andreani, D. Peyrade, Y. Chen, Opt. Express 16 (2008) 11624.
[11] K. Nozaki, T. Tanabe, A. Shinya, S. Matsuo, T. Sato, H. Taniyama, M. Notomi, Nat. Photon. 4 (2010) 477.
[12] M. Belotti, M. Galli, D. Gerace, L.C. Andreani, G. Guizzetti, A.R. Md Zain, N.P. Johnson, M. Sorel, R. De La Rue, Opt. Express 18 (2010) 1450.
[13] M. Galli, D. Bajoni, M. Patrini, G. Guizzetti, D. Gerace, L. Andreani, M. Belotti, Y. Chen, Phys. Rev. B 72 (2005) 125322.
[14] C. Sauvan, G. Lecamp, P. Lalanne, J.-P. Hugonin, Opt. Express 13 (1) (2005) 245.
[15] A. Taflove, Computational Electrodynamics: The Finite-Difference Time-Domain Method, third ed., Artech House, Boston, 2005.
[16] E.D. Palik (Ed.), Handbook of Optical Constants of Solids, Academic Press, New York, 1985.
[17] M.I. Stockman, Phys. Rev. Lett. 93 (2004) 137404.
[18] S. Kawata, M. Ohtsu, M. Irie (Eds.), Nano-Optics, Springer, Berlin, 2002.
[19] U. Fano, Phys. Rev. 124 (1961) 1866.
[20] A.E. Miroshnichenko, S. Flach, Yu.S. Kivshar, Rev. Mod. Phys. 82 (2010) 2257.
[21] M.I. Tribelsky, S. Flach, A.E. Miroshnichenko, A.V. Gorbach, Yu.S. Kivshar, Phys. Rev. Lett. 100 (2008) 043903.
[22] M. Galli, S.L. Portalupi, M. Belotti, L.C. Andreani, L. O'Faolain, T.F. Krauss, Appl. Phys. Lett. 94 (2009) 07101.
[23] J. Merlein, M. Kahl, A. Zuschlag, A. Sell, A. Halm, J. Boneberg, P. Leiderer, A. Leitenstorfer, R. Bratschitsch, Nat. Photon. 2 (2008) 230.